

<연구논문>

Fabrication of Metal-based and AlGaAs/GaAs-based Mesoscopic Ring Structures and Characterization of their Quantum Interference Phenomena

KyoungWan Park, Seongjae Lee, Mincheol Shin, El-Hang Lee,
Ju-Jin Kim* and Hu Jong Lee*

Electronics and Telecommunications Research Institute, Daejeon 305-606, Korea

**Pohang Institute of Science and Technology, Pohang 790-600, Korea*

(Received July 9, 1993)

금속과 AlGaAs/GaAs의 중시적 고리구조의 제작 및 양자간섭 현상의 측정

박경완 · 이성재 · 신민철 · 이일항 · 김주진* · 이후종*

한국전자통신연구소, *포항공과대학

(1993년 7월 9일 접수)

Abstract – We have fabricated metal-based Aharonov-Bohm ring structures by using electron beam lithography and lift-off techniques and examined various quantum interference phenomena resulting from wave natures of electrons. Oscillations of magnetoresistance were observed at low temperatures, which we attribute to quantum interference and coherent back scattering effect of normal electrons. The intensity of aperiodic fluctuation was measured and explained by the general formula of the conductance fluctuation. Non-local behavior of the electron transport involving the reciprocity relation in the magnetoresistance was seen in the ring structures. Also, mesoscopic rings from the modulation-doped AlGaAs/GaAs heterostructures have been fabricated by using electron beam lithography and chemical wet etching techniques. The magnetoresistance has been measured at 10 mK in order to examine the transport characteristics in the regime where the quantum effects and the ballistic transport dominate.

요 약 – 전자의 파동성에 기인하는 여러가지 양자간섭 현상을 연구하기 위하여, 금속의 미세고리구조를 제작하였다. 전자의 양자간섭과 가간섭 역충돌 효과에 의한 자기저항의 진동현상이 관측되었으며, 자기저항의 비주기 섭동 현상과 비국재현상도 관찰되어 중시적 전기 전도도의 일반식에 의하여 설명되었다. 또한 AlGaAs/GaAs의 이차원 전자가스층을 이용한 고리구조도 제작되어, 양자효과와 탄동적 수송의 영역에서 자기저항이 측정되었다.

1. Introduction

Recent advancement in microfabrication technology has allowed fabrication of a variety of lateral quantum structures, called “mesoscopic”, where the electrical properties should be described by the quantum mechanics [1]. The study of such structure

has been the focus in both basic physics and device applications [2]. The critical dimension is comparable to the inelastic scattering length of electrons ($L_0 = (D\tau)^{1/2}$, D = the diffusion constant, τ = mean time between inelastic scatterings), so that various wave natures of electrons can be explored. For the study of quantum transport in a single wire,

the most important dimension is the length of the wire which has to be smaller than L_ϕ . For Aharonov-Bohm (A-B) study [3], the perimeter of the ring structure should be less than L_ϕ . The ratio of the channel width to the ring diameter is another important factor, since the magnetic field enclosed by the ring produces periodic oscillations in the magnetoresistance, while the field piercing the channels produces aperiodic fluctuations. There are several quantum resistance behaviors in the mesoscopic structures, such as quantum interference and nonlocal behavior. The critical dimensions of mesoscopic structure have been discussed elsewhere [4].

Investigations of the A-B effect [5], the coherent back scattering effect [6], and the conductance fluctuation [7], originated from the phase interference of normal electrons in the mesoscopic structures, have been conducted in normal metals and semiconductor heterostructures [8]. In the A-B effect experiment, the path of electrons is split into two channels and then recombined. If the coherence is maintained between two channels, the interference effect can be observed. The magnetic flux enclosed by the loop shifts the relative phase defined by $\phi = 2\pi e/h \int B \cdot ds$. The change of h/eS in magnetic field where S is the average area of the ring, yields change of 2π in the relative phase, and this phase shift results in the conductance oscillations. In the mesoscopic ring structure, there is a possibility that the electron waves can be scattered back to the initial point along the closed path in the loop and scattered back along the same path in the reverse direction (weak localization effect) [9]. When the coherent back scattering effect exists, the period of the conductance oscillation is $h/e (2S)$ in magnetic field because the electron wave travels the entire loop.

The magnetoresistances of mesoscopic samples showed random fluctuations which are reproducible. This behavior results from the quantum mechanical interference of the electron wavefunctions. The superpositions of the wavefunctions depend on the impurity configuration, on magnetic field, and on the driven current. The fluctuations always have amplitudes of $\Delta G \sim e^2/h (E_c/kT)^{1/2} (L_\phi/L)^{3/2}$, $E_c = \hbar D/L_\phi^2$ [10]. The amplitude of the fluctuations decreased as the sample dimension became larger than

the coherence length.

Since electron wavefunctions extend over the region of mesoscopic size L_ϕ , the properties of electron are not classical, local objects. Therefore, the conductance contains non-local behaviors [11]. For instance, the conductance is not zero far from the classical current paths through the sample. Neither it is symmetric under the reversal of the magnetic field, which is called the reciprocity relation [12, 15].

Mesoscopic structures in the semiconductor heterojunction having high mobility are expected to show a variety of quantum mechanical phenomena associated with electron interference. Recently, there has been growing interest in understanding the transport characteristics in the regime where the quantum effects and the ballistic transport mechanism dominate. The two-dimensional electron gas (2DEG) at AlGaAs/GaAs heterojunction has both elastic and inelastic scattering lengths of several microns. Extensive studies of electron interference effects as well as quantization of resistance and a phase preserving electron wave guide, have been done by confining the 2DEG to a narrow conducting channel [13].

We have used electron beam lithography and lift-off technique/chemical wet etching technique to produce the metal/semiconductor A-B ring structures. Transport measurements exhibited the A-B interference and coherent back scattering effects, conductance fluctuation, and nonlocal resistance behavior in magnetoresistance spectra.

2. Fabrication of Aharonov-Bohm Ring Structures and Measurement of Magnetoresistance

In order to investigate the quantum interference effects of normal electrons, test structures of metal (Sb and Al) and 2DEG AlGaAs/GaAs heterostructure were fabricated as shown in Fig. 1. The metal ring structures were fabricated on a 1000 Å thick silicon oxide layer which was thermally grown on a silicon substrate by electron beam lithography at 30 kV. The electron beam exposure was done to the polymethylmethacrylate (PMMA) resist layer

with a total thickness of about 400 nm on the silicon oxide, followed by a lift-off of 30 nm thick Sb and Al. It consists of a closed square loop with dimensions of 0.8 by 0.8 μm and a linewidth of 0.2 μm . And semiconductor ring structures were fabricated on the 2DEG AlGaAs/GaAs heterostructure which

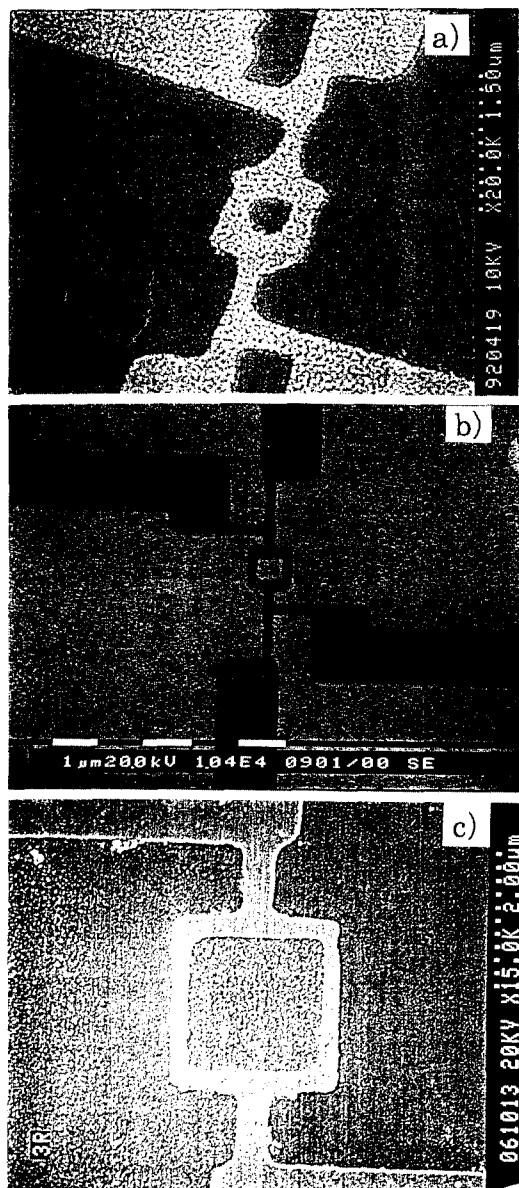


Fig. 1. Scanning electron micrographs of (a) Sb, (b) Al, and (c) two dimensional electron gas from AlGaAs/GaAs heterostructure Aharonov-Bohm loop structures.

was grown by molecular beam epitaxy (MBE). The electron beam exposure was done to a polymer (SAL) resist layer with a total thickness of about 400 nm on the substrate, followed by a chemical wet etching ($\text{H}_3\text{PO}_4 : \text{H}_2\text{O}_2 : \text{H}_2\text{O}$) of the modulation doped AlGaAs layer. It consists of a closed square loop with dimensions of 2.5 by 2.5 μm and a linewidth of 0.4 μm .

Dilution refrigerator with a superconducting magnet was used in order to measure the magnetoresistance. We calculated the resistances from the voltages measured by the four-point probe method. Lock-in amplifier measurement technique with low frequency AC current (10^{-9} Ampere) was used to improve the signal-to-noise sensitivity, while the magnetic field was swept at 200~300 gauss/min.

3. Results and Discussion

Two sets of the magnetoresistance curves in a large magnetic field ranging from 0 to 3 Tesla, are shown in Fig. 2 and Fig. 3 for Sb and Al loops, respectively. All curves are offset for clear display and zero-field resistances of the loops are 420 Ω for Sb and 8.85 Ω for Al. Both figures display noise-like patterns generally known for the conductance fluctuation [7]. But it differs from the thermal noise, because it is reproducible. It is also called "magnetic fingerprint", since it depends on the microscopic configuration of the elastic scattering centers in the

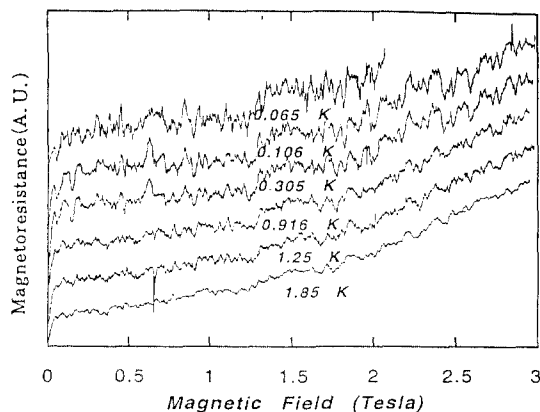


Fig. 2. Magnetoresistance spectra of the Sb sample at different temperatures.

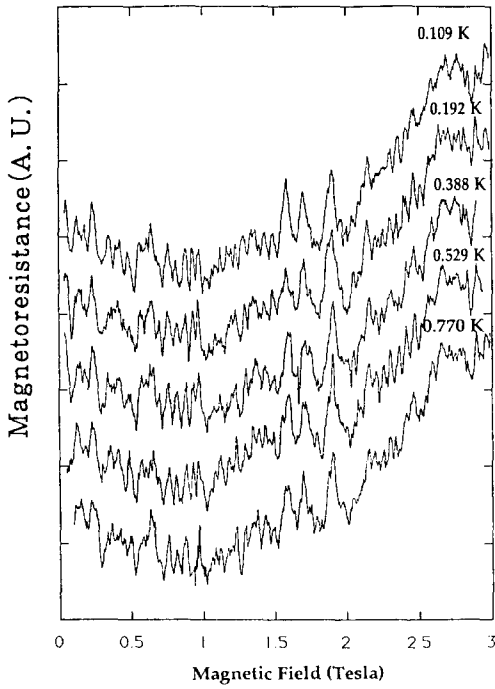


Fig. 3. Magnetoconductance spectra of the Al sample at different temperatures.

coherent region of a sample [14]. The reproducibility has been checked and confirmed well for both samples.

Several observations in the magnetoconductance curves for Sb and Al rings need to be discussed. In Fig. 2, the fluctuations in Sb sample are seen to grow gradually as we lower the temperature, and superposed on the nearly temperature-independent background. In order to inspect them in more detail, nine curves at different temperatures are shown in Fig. 4. Nearly monotonic behavior is transformed into the rapidly changing one with many peaks and valleys as the temperature decreases. Especially, small peaks on the large signal are seen with a period which corresponds to that of A-B oscillations at $T=65$ mK. Otherwise, the large signals have no periodicity (aperiodic fluctuation). In order to show the periodicity more clearly, the Fourier transformation spectrum of these data is plotted in Fig. 5(a). The peak pointed by an arrow reflects the A-B h/e oscillation, since the estimated diameter of $0.8 \mu\text{m}$ from the peak position at $108 T^{-1}$ agrees well with the average diameter of the Sb ring measured by

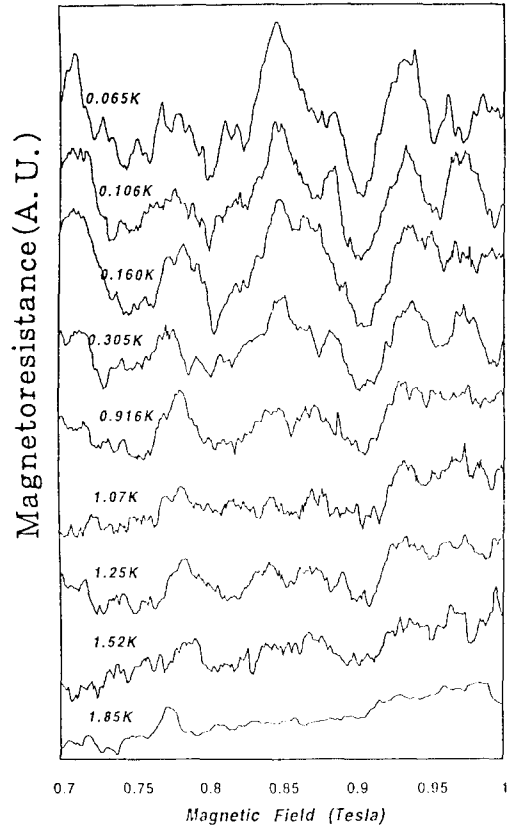


Fig. 4. Magnetoconductance spectra of the Sb sample in the magnetic field of 0.7~1.0 T.

scanning electron microscope [The same type of h/e oscillation is also observed in the Al sample and shown in Fig. 5(b)]. The temperature dependence of the fluctuation amplitude has been investigated, and the relation is found to be $\Delta G \sim T^{-1/2}$. The magnitudes of the fluctuation estimated from the relation of $\Delta G \sim O(1) e^2/h$ also agree well with the theory on the universal conductance fluctuation (UCF) [10].

Compared with the Sb sample, the Al sample shows a quite different behavior as illustrated in Fig. 3. First, fluctuations are nearly temperature-independent both in magnitude and shape. It means that the electron's phase-coherent length, L_ϕ , is comparably larger than the sample's dimension of about $2 \mu\text{m}$ in the temperature range explored. The magnitude of the conductance fluctuations is $\sim 0.5 e^2/h$, which is larger than that of Sb sample. Secondly, the fluctuations are superposed on a nearly tempe-

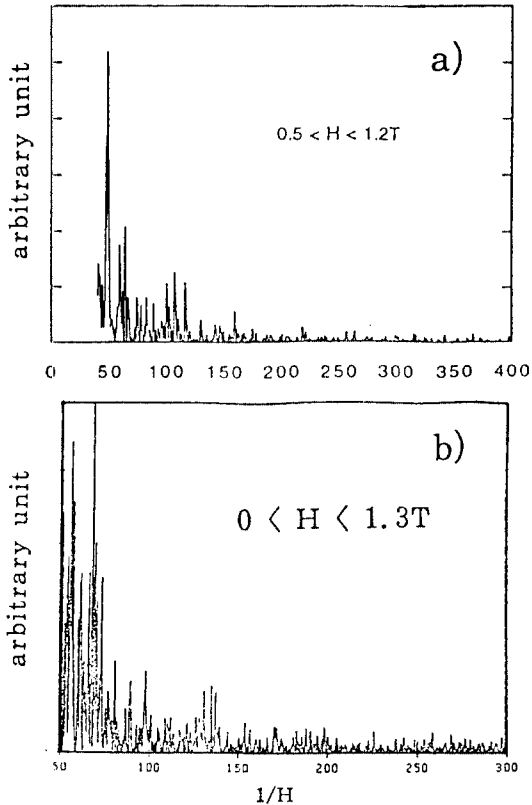


Fig. 5. Fourier transformation spectrum of the magnetoresistance of Sb-sample at 65 mK. The magnetic field was swept in the range of 0.5~1.2 T (a). Fourier transformation spectrum of the magnetoresistance of Al-sample at 65 mK. The magnetic field was swept in the range of 0~1.3 T (b).

perature-independent background magnetoresistance, which has a dip centered at $B=1$ Tesla. To see it more clearly, we changed the direction of the field and obtained data given in Fig. 6. It is obvious that we have a parabolic background which, however, is not symmetric about $B=0$, but about $B=1$ Tesla. It can be explained by the geometry employed for the measurements as can be seen in Fig. 1; Hall resistance which is proportional to B is added to the longitudinal one which is proportional to B^2 .

Due to a large electron phase coherent length we can expect the manifestation of the reciprocity relation put forward by Buttiker [15] which is noted as the equation; $R_{12,34}(B)=R_{34,12}(-B)$. This relation is well demonstrated in Fig. 7 for the Al loop. It

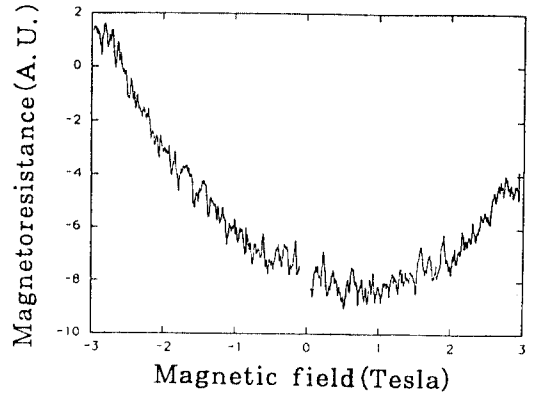


Fig. 6. Magnetoresistance spectrum of the Al-sample at 0.109 K.

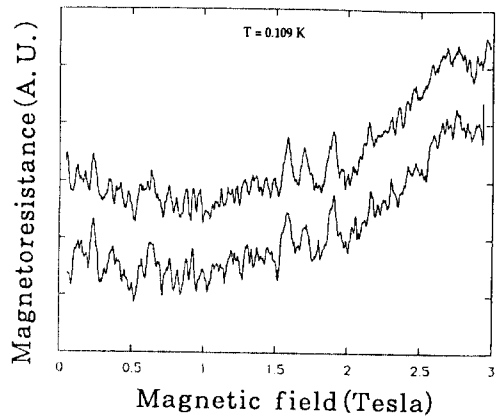


Fig. 7. Reciprocity relation of magnetoresistance of the Al-sample at 0.109 K.

verifies the fact that electrons in the Al loop move coherently during multiple elastic scatterings to preserve a time-reversal symmetry included in the Hamiltonian.

Al becomes a superconductor below the transition temperature of 1.14 K and the critical field of 105 Gauss. Our sample shows the superconductivity at zero field below 1.20 K. At temperatures above the superconducting transition, we have observed $h/2e$ oscillation (AAS oscillation) [6] which is not shown here. It develops into the Little-Parks oscillation [16] as the normal state changes over to the superconducting one. Moreover, we have observed a resistance anomaly in the mesoscopic Al loop near the superconducting transition regime [17], which will be discussed in a separate paper [18]. Compared

with normal electron properties, mesoscopic superconducting system have attracted less attention. Recently, several theoretical and experimental investigations have appeared in analogy to the mesoscopic effects in the normal state [19].

Mesoscopic rings from the modulation-doped AlGaAs/GaAs heterostructure have been fabricated by using electron beam lithography and chemical wet etching techniques (Fig. 1). We have measured the magnetoresistance at 10 mK in order to study the transport characteristics in the regime where quantum effects and ballistic transport dominate. It was observed that the quantum interference signal was superposed on the mixture of Shubnikov de Haas oscillations and quantum Hall plateaus, and the intensity decreased at high magnetic fields. The results will be reported in a separate paper in detail.

In summary, We have fabricated metal-based and AlGaAs/GaAs-based Aharonov-Bohm ring structures and examined various quantum interference phenomena resulting from wave natures of electrons.

This research has been supported in part by Korea Telecomm.

References

1. B. L. Altshuler, P. A. Lee and R. A. Webb, *Mesoscopic Phenomena in Solids*, (North-Holland, 1990). The concept of "mesoscopic" is described therein.
2. (a) M. A. Reed and W. P. Kirk, *Proc. of the Intl. Sym. of Nanostructure Physics and Fabrication*, (Academic Press, Inc., San Diego, 1990); (b) H. Koch and H. Lubbig, *Single Electron Tunneling and Mesoscopic Devices*, (Springer-Verlag, 1991). Many examples are in these proceedings.
3. Y. Aharonov and D. Bohm, *Phys. Rev.* **115**, 485 (1956).
4. H. Schmid, S. A. Rishton, D. P. Kern, S. Washburn, R. A. Webb, A. Kleinsasser and T. H. P. Chang, *J. Vac. Sci. Technol.* **B6**, 122 (1988).
5. (a) R. A. Webb, S. Washburn, C. P. Umbach, and R. B. Laibowitz, *Phys. Rev. Lett.* **54**, 2696 (1985); (b) S. Washburn and R. A. Webb, *Adv. Phys.* **35**, 375 (1986).
6. V. Chandrasekher, H. J. Rooks, S. Wind and D. E. Prober, *Phys. Rev. Lett.* **55**, 1610 (1985).
7. (a) A. D. Stone, *Phys. Rev. Lett.* **54**, 2692 (1985); (b) A. D. Stone and Y. Imry, *Phys. Rev. Lett.* **56**, 189 (1986).
8. (a) S. Washburn, H. Schmid, D. Kern and R. A. Webb, *Phys. Rev. Lett.* **59**, 1791 (1987); (b) P. M. Mankiewich, R. E. Behringer, R. E. Howard, A. M. Chang, T. Y. Chang, B. Chelluri, J. Cunningham and G. Timp, *J. Vac. Sci. Technol.* **B6**, 131 (1988); (c) K. Ishibashi, T. Takagaki, K. Gamo, S. Namba, S. Takaoka, K. Murase, S. Ishida, Y. Aoyagi, *J. Vac. Sci. Technol.* **B6**, 1852 (1988).
9. S. Hikami, A. Larkin and Y. Nagaoka, *Prog. Theor. Phys.* **63**, 707 (1980).
10. F. P. Milliken, S. Washburn, C. P. Umbach, R. B. Laibowitz and R. A. Webb, *Phys. Rev.* **B36**, 4465 (1987).
11. C. P. Umbach, P. Santhanam, C. van Haesendonck and R. A. Webb, *Appl. Phys. Lett.* **50**, 1289 (1987).
12. S. Komiyama, H. Hirai, S. Sasa and F. Fujii, *Surf. Sci.* **229**, 224 (1990).
13. (a) G. Timp, A. M. Chang, P. deVegvar, R. E. Howard, R. Behringer, J. E. Cunningham and P. M. Mankiewich, *Surf. Sci.* **196**, 68 (1988); (b) G. Timp, P. M. Mankiewich, P. deVegvar, R. Behringer, J. E. Cunningham, R. E. Howard and H. U. Baranger, *Phys. Rev.* **B39**, 6227 (1989).
14. S. Washburn, *J. of Research and Development* **32**, 335 (1988).
15. M. Buttker, *Nanostructured Systems*, (Academic Press, Inc., 1992), Edited by M. Reed, p. 191.
16. W. A. Little and R. D. Parks, *Phys. Rev. Lett.* **9**, 9 (1962).
17. P. Santhanam, C. C. Chi, S. J. Wind, M. J. Brady, and J. J. Bucchignano, *Phys. Rev. Lett.* **66**, 2254 (1991).
18. in preparation.
19. (a) P. Santhanam, C. P. Umbach, and C. C. Chi, *Phys. Rev.* **B40**, 11392 (1989); (b) H. Vloeberghs, V. V. Moshchalkov, C. Van Haesendonck, R. Jonckheere and Y. Bruynseraede, *Phys. Rev. Lett.* **69**, 1268 (1992); (c) V. T. Petrashov, V. N. Antonov, P. Delsing and R. Claeson, *Phys. Rev. Lett.* **70**, 347 (1993).